γ-ray production by inelastic proton scattering on ^{16}O and ^{12}C

J. Kiener,[1] M. Berheide,[1] N. L. Achouri,[2] A. Boughrara,[3] A. Coc,[1] A. Lefebvre,[1] F. de Oliveira Santos,[4] and Ch. Vieu[1]
[1]*CSNSM, IN2P3-CNRS, Bâtiments 104 et 108, F-91405 Campus Orsay, France*
[2]*LPC-ISMRa, Boulevard du Maréchal Juin, 14050 Caen Cedex, France*
[3]*USTHB, Institut de Physique, Boîte Postal 32, 16111 Bab Ezzouar, Algiers, Algeria*
[4]*GANIL, IN2P3-CNRS, IRF-CEA, Boîte Postal 5027, 14021 Caen Cedex, France*
(Received 16 April 1998)

Excitation functions for the production of the 2.74, 6.13, 6.92, and 7.12 MeV γ rays by inelastic proton scattering on ^{16}O have been measured in steps of 200–500 keV for proton energies $E_p = 8.4–20$ MeV. For the 4.44 MeV γ rays of ^{12}C produced by inelastic proton scattering on ^{12}C data have been obtained for proton energies $E_p = 8.4–14$ MeV and at $E_p = 17.25$, 18.25, and 19.75 MeV. Eight high efficiency Ge detectors with anti-Compton shielding for the γ-ray detection were used to obtain the laboratory γ-angular distributions. The results of Legendre polynom fits to these distributions are discussed and presented in suitable form for use in γ-ray astronomy. [S0556-2813(98)02310-3]

PACS number(s): 25.40.Ep, 23.20.En, 26.40.+r

I. INTRODUCTION

Interactions of accelerated nuclei of medium-high energy with the surrounding material in astrophysical sites can be revealed by the induced γ radiation. The characteristic γ-ray spectra from such scenarios have been up to date unambiguously observed from solar flares and also very recently from the direction of the Orion molecular cloud complex and more observations may be forthcoming in the near future thanks to the substantial number of satellites equipped with γ detectors, already in orbit or soon to be launched. These γ-ray spectra yield important information on the elemental composition and physical conditions of the interaction site and on the spectrum and composition of the accelerated particles. Among the most prominent features in solar flare spectra are the deexcitation lines of the first excited state in ^{12}C at 4.44 MeV and the second excited state in ^{16}O at 6.13 MeV (see, e.g., Ref. [1]). The spectra taken by the Comptel detector on board of the Compton Gamma Ray Observatory in the direction of the Orion clouds [2] can even be understood by considering only the deexcitation of these two nuclei [3,4].

In both scenarios inelastic scattering of protons and α particles on C and O nuclei at energies below $E/A = 100$ MeV is responsible for an important part of the observed γ-ray line emission. A good knowledge of the γ-production cross sections, induced by inelastic scattering, is therefore needed for the interpretation of the spectra. Although a lot of experimental and theoretical work on the cross sections is accomplished (for an overview see [5]), Tatischeff *et al.* [6] pointed out the need for experimental data of the ^{16}O(p,p') and ^{16}O(α,α') reactions below $E/A = 100$ MeV producing the 6.92 and 7.12 MeV γ rays. In particular, it was shown that a precise determination of the ratios of the 6.13, 6.92, and 7.12 MeV deexcitation lines could yield valuable information about the energy spectrum of the accelerated nuclei.

Another important point for the correct interpretation of the observed γ-ray spectra is the angular distribution of the γ radiation. In the deexcitation of energetic nuclei, even with uniformly distributed velocity vectors in space, γ rays emitted at angles corresponding to the maxima of the γ-angular distribution in the rest frame of the nucleus will be preferentially detected. The Doppler shift may then lead to several distinct maxima in this broad line scenario. Bykov *et al.* [7] have calculated those broad line spectra for the 4.44 and 6.13 MeV deexcitation lines of ^{12}C and ^{16}O, respectively. Kozlovsky *et al.* [8] extended the calculations to anisotropic interaction scenarios where energetic ^{12}C and ^{16}O nuclei impinging on the Orion molecular clouds have a preferential direction with respect to our line of sight. Such scenarios could be responsible for the observed energy shift and possible line splitting in the Comptel spectra of Orion and are also expected in solar flares. Experimental data of γ-angular distributions are, however, still more scarce than cross section data.

We measured excitation functions for the ^{16}O$(p,p\gamma)^{16}$O reaction in small energy steps of 200 to 500 keV for proton energies between 8.4 and 20 MeV. Laboratory angular distributions for the 2.74 MeV (2^-, 8.87 MeV $\rightarrow 3^-$, 6.13 MeV), 6.13 MeV (3^-, 6.13 MeV $\rightarrow 0^+$, g.s.), 6.92 MeV (2^+, 6.92 MeV $\rightarrow 0^+$, g.s.), and 7.12 MeV (1^-, 7.12 MeV $\rightarrow 0^+$, g.s.) deexcitation γ rays of ^{16}O have been obtained in that experiment. Cross sections and angular distribution coefficients, obtained from Legendre polynom fits to the data are presented for the four γ-ray transitions in the whole above-mentioned proton energy range. Absolute cross sections are deduced by normalizing the data to the 6.13 MeV data of Dyer *et al.* [9]. Additionally, angular distributions for the 4.44 MeV deexcitation γ ray in ^{12}C (2^+, 4.44 MeV $\rightarrow 0^+$, g.s.) from the ^{12}C$(p,p\gamma)^{12}$C reaction have been obtained for proton energies $E_p = 8.4–14$ MeV and at 17.25, 18.25, and 19.75 MeV. Finally, to facilitate the use of the data in γ-ray astronomy, energy averaged data over 1 MeV are presented in tabular form.

II. EXPERIMENT

The experiment was done at the Tandem accelerator of the Institute of Nuclear Physics at Orsay. A pulsed proton

beam of 0.5–2 nA intensity was directed onto the target, situated in a tubular reaction chamber of 5×5 cm^2 cross section equipped with a plastic window facing the γ detectors. The beam current was integrated in a Faraday cup, located 3 m behind the reaction target. The beam position and spot size were controlled optically before each run with two plastic scintillators situated 1 m upstream and downstream of the target.

The induced γ rays were detected by a set of eight high efficiency ($\epsilon=80\%$) HP-Ge detectors with BGO shielding for Compton suppression from the Eurogam phase I setup [10]. The Ge crystals were placed at 23 cm distance from the target at six different angles with respect to the beam direction. The relative efficiency for different γ-ray energies was determined from a measurement with a calibrated ^{207}Bi source and a calibrated composite ^{238}Pu-^{13}C source. A function extracted from an efficiency measurement for γ energies from 0.66 to 10.6 MeV for those detectors at the same target distance with the ^{27}Al(p,γ) reaction [11] was fit to the four data points given by the two calibration sources using a single calibration factor for each detector. The fits resulted in an error of less than 3% for the individual detector efficiencies, with an overall systematic error of 9% due to the uncertainty in the source activities.

Several target foils were used during the experiment. In a first series of measurements a tantalum oxide target of 500 μg/cm^2 evaporated on a carbon backing was used for proton energies from 8.4 to 12.2 MeV. Above this energy, γ rays resulting from reactions with the Ta nuclei become too intense. The target stability was verified by regular measurements at a proton energy of 10 MeV. No deterioration of the target during proton irradiation was observed. In a second series three different self-supporting collodion foils (chemical composition $C_{12}H_{16}N_4O_{18}$) of thickness 0.7–3.5 mg/cm^2 were used for measurements with proton energies ranging from 8.6 to 20 MeV. With these targets a typical loss of the oxygen content of 50% in 12 h irradiation with 0.5 nA proton beams was observed.

The carbon content in both target materials allowed us to obtain also γ-angular distributions for the 4.44 MeV transition in ^{12}C from $E_p=8.4$ MeV up to an energy, where the 4.44 MeV γ-ray production from ^{16}O$(p,p\alpha\gamma)^{12}$C stays negligible compared to the production of this γ ray from inelastic proton scattering on ^{12}C. This energy is estimated to be 14 MeV from the data of Dyer *et al.* [9]. The contribution of the ^{14}N$(p,^3$He$\gamma)^{12}$C reaction to the 4.44 MeV γ rays with the collodion targets is estimated from [12,13] to be less than 15% below 14 MeV. Additionally we used a carbon target of 246 μg/cm^2 for three proton energies: $E_p=17.25$, 18.25, and 19.75 MeV. The γ-angular distribution for the 2.31 MeV transition in ^{14}N was obtained with the collodion target. This distribution is isotropic due to spin zero of the excited state and could thus be used as a check of the relative efficiency calibration of the different Ge detectors.

For each event the energy signal and the time difference between the detector signal and the beam pulse were recorded in list mode. The timing signal was used to discriminate against neutron induced signals in the detectors and against γ rays originating from beam interactions with collimators and in the Faraday cup. When gating into the prompt peak the remaining background contribution from the above-

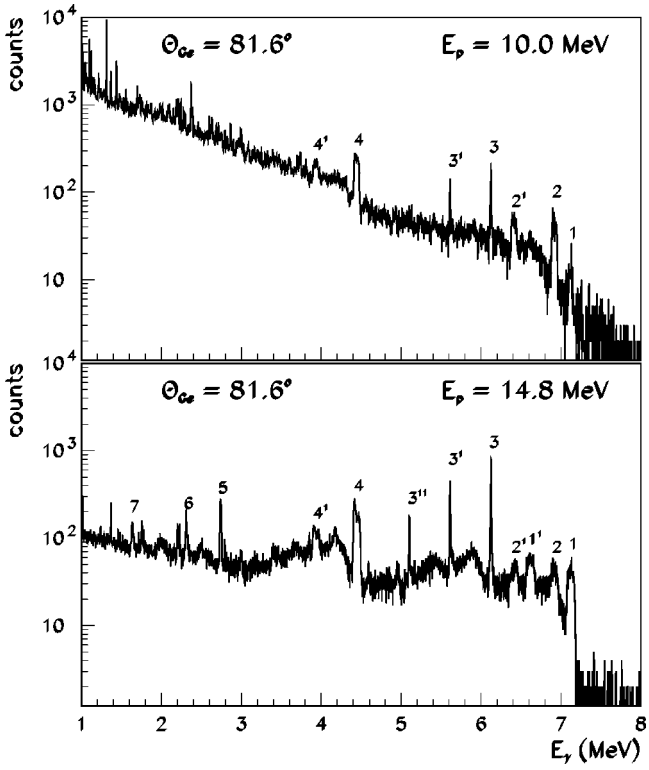

FIG. 1. γ-energy spectra with the tantalum-oxide target (upper figure) and the collodion target (lower figure) observed by the Ge detector at 81.6°. Several important lines are labeled by numbers. The corresponding transitions are (1) ^{16}O 7.12 MeV $\rightarrow$ g.s., (2) ^{16}O 6.92 MeV $\rightarrow$ g.s., (3) ^{16}O 6.13 MeV $\rightarrow$ g.s., (4) ^{12}C 4.44 MeV $\rightarrow$ g.s., (5) ^{16}O 8.87 MeV $\rightarrow$ 6.13 MeV, (6) ^{14}N 2.31 MeV $\rightarrow$ g.s., (7) ^{14}N 3.95 MeV $\rightarrow$ 2.31 MeV. First and second escape peaks are labeled by the superscripts 1 and 11, respectively. The peak widths and shapes depend on the energy and angular distribution of the recoiling nuclei and their slowing down in the target material, the γ-angular distribution, and the lifetime of the excited states. The narrow lines of the 6.13 MeV transition in ^{16}O $(3,3^1,3^{11})$ reflect approximately the detector energy resolution.

mentioned processes to the lines at 2.74, 4.44, 6.13, 6.92, and 7.12 MeV is estimated to be less than 1% at all proton energies. Typical energy spectra with the tantalum oxide target and the collodion target are shown in Fig. 1. For some important lines, the γ transitions are marked.

III. DATA ANALYSIS

Data for the γ-angular distributions were obtained by integrating the surface of the different peaks of interest in the energy calibrated spectra. Approximate peak shapes for a guide to the integration were obtained by a Monte Carlo simulation of the experiment. This was especially important for the 6.13 MeV line of ^{16}O, where a small fraction of the γ rays are emitted in flight and form a tail beneath the more intense and narrow peak from the γ rays emitted at rest ($t_{1/2}=18.4$ ps). For all other transitions, the lifetime of the excited state is much shorter ($t_{1/2}=4.7-125$ fs) and practically all γ rays are emitted in flight. There the simulation helped in determining the line boundaries in some cases.

The background was estimated for each peak individually and taken as a straight line adjusted to the count rates in the

regions below and above the peaks. The systematic error due to this background evaluation was estimated to be generally of the order of the statistical error, however, with some exceptions for the 6.92 and 7.12 MeV lines. For the 6.13 MeV line this error is typically 1–4 % with the collodion target and 4–10 % with the tantalum-oxide target. For the detectors at forward angles, the second escape peak of the 7.12 MeV γ rays has some overlap with the 6.13 MeV line, but is strongly reduced thanks to the Compton suppression. It amounted to max 5% of the 6.13 MeV line. This has been included in the background subtraction. For the 6.92 and 7.12 MeV lines the estimated systematic error due to background subtraction is typically 3–5 % but increases up to 50% at some beam energies where the background subtraction became very uncertain, especially for the tantalum-oxide target at proton energies above 11 MeV. Typically 3.5–8, 2–8, and 1–2.5 % are estimated for the 2.31, 2.74, and 4.44 MeV line, respectively. These errors were linearly added to the error of 3% in the determination of the individual detector efficiencies and to the usual statistical error from the quadratic sum of the errors of the total count rate and the background count rate.

The obtained laboratory γ-angular distributions were then fitted by a Legendre polynom

$$W(\Theta)=\sum_{l=0}^{l=l_{\max}} a_l \; Q_l \; P_l(\cos\Theta) \quad (l \;\; \text{even}) \qquad (1)$$

with $l_{\max}=0$ for the 2.31 MeV line (spin and parity of the excited state: 0^+), $l_{\max}=2$ for the 2.74 MeV ($M1$ transition) and 7.12 MeV ($E1$ transition) lines, $l_{\max}=4$ for the 4.44 MeV and 6.92 MeV line ($E2$ transition) and $l_{\max}=6$ for the 6.13 MeV line ($E3$ transition). The Q_l are the attenuation coefficients, which can be calculated analytically for the actual detector setup (see, for example, [14]). Examples of angular distribution fits are shown in Fig. 2.

Absolute cross sections have been obtained by normalizing the data to the excitation functions of Dyer *et al.* [9] for the production of the 4.44 and 6.13 MeV γ rays by inelastic proton scattering on ^{12}C and ^{16}O, respectively. For the tantalum-oxide target, the overall nominal target thickness was known, but a partial deoxydation of the tantalum-oxide was observed during the evaporation process, which made the oxygen content uncertain. Comparison with the 6.13 MeV data of Dyer *et al.* [9] and repeated runs at the same beam energy showed the stability of this target with respect to proton irradiation. Finally, an overall correction factor with respect to the nominal oxygen content, determined by comparison with the 6.13 MeV Dyer *et al.* data at $E_p=11.2-11.8$ MeV, where the excitation function shows a plateau, was applied for the absolute cross section determination with that target. For the three different collodion targets we used, a rapid and irregular degradation of the target was observed, independent of proton energy. Therefore, absolute cross sections could not be obtained with these targets. Thus, for each proton energy we normalized the cross sections of the 6.13 and 4.44 MeV data to the Dyer *et al.* data and applied then the same normalization factor to the 2.74, 6.92, and 7.12 MeV data. This normalization factor was obtained by averaging the Dyer *et al.* cross section using a linear interpolation between their data points over the proton energy loss in the target. This procedure results in an additional error in the region of the narrow resonances due to an uncertainty in the incoming proton beam energy, estimated to be 60 keV, which was added to the error of the extracted cross section as explained above. As the main goal of that experiment was the determination of energy integrated relative cross sections of the 7.12, 6.92, 6.13, and 2.74 MeV γ rays and γ-angular distributions for γ-ray astronomy, no further efforts were made to obtain independent absolute cross section determinations.

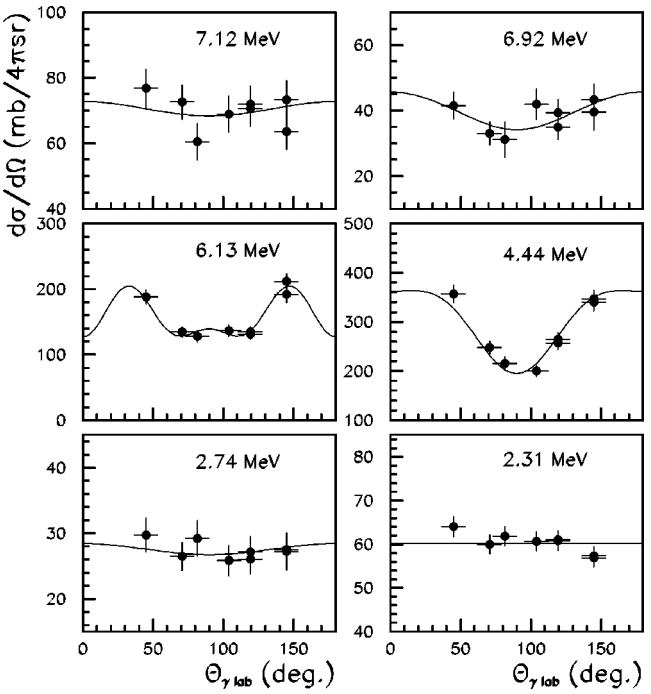

FIG. 2. γ-angular distributions obtained at a proton energy $E_p=14$ MeV, except for the 2.31 MeV line, where the sum of all (30) runs with one of the collodion targets is shown ($E_p=9-20$ MeV). The vertical error bars contain the statistical error and the error of the detector efficiency. The horizontal error bars correspond to the opening angle of the detectors. The solid curves are Legendre polynom fits to the data.

IV. RESULTS AND DISCUSSION

Excitation functions of the γ-angular distributions from the ^{16}O$(p,p\gamma)^{16}$O reaction for $E_\gamma=2.74$, 6.13, 6.92, and 7.12 MeV and of the ^{12}C$(p,p\gamma_{4.44})^{12}$C reaction are displayed in Figs. 3–7. The main result of this study is the measurement of the complete excitation function between $E_p=8.4$ MeV and 20 MeV for the ^{16}O$(p,p\gamma_{2.74,6.92,7.12})^{16}$O reactions and the determination of the γ-angular distribution in the same energy range of the ^{16}O$(p,p\gamma_{6.13})^{16}$O reaction. It is interesting to compare the γ-production cross sections with inelastic scattering cross sections. Dangle *et al.* [15] measured excitation functions for the ^{16}O$(p,p')^{16}$O$^*_{6.13,6.92,7.12}$ inelastic scattering reactions between $E_p=7.3$ and 10.5 MeV. In this energy range, contributions from higher lying levels are completely negligible for the above-mentioned γ rays. Therefore and because of a 100% branching to the ground state for the three levels, inelastic scattering cross sections and γ-production cross sec-

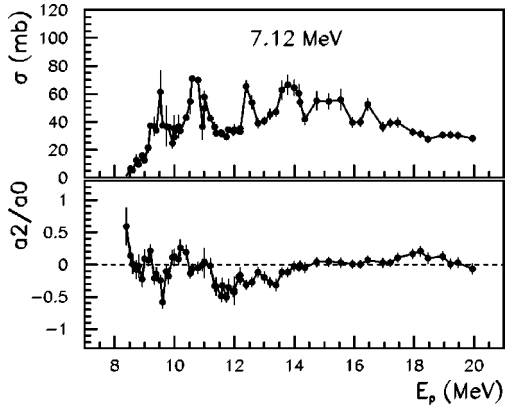

FIG. 3. Excitation function of the $^{16}O(p,p\gamma_{7.12})^{16}O$ reaction. The error bars on the cross section include the error of the Legendre polynom fit and for the data taken with the collodion targets an additional error from the normalization procedure (see text). This normalization with respect to the 6.13 MeV data of Dyer *et al.* [9] results in somewhat larger error bars for data points obtained with the collodion targets in the region of the narrow resonances below 12 MeV compared to the data points obtained with the tantalum-oxide target. At higher energy the excitation function for the 6.13 MeV γ-ray production gets smooth and the error due to the relative normalization to the Dyer *et al.* data is reduced compared to the usual error from the Legendre polynom fit. The error on the other coefficients is the error from the Legendre polynom fit.

tions must be the same. The inelastic scattering cross sections are actually in very good agreement (to better than 10%) with the respective γ-production cross sections. This confirms the absolute normalization of the 6.13 MeV Dyer *et al.* data, which are also in agreement with the data of

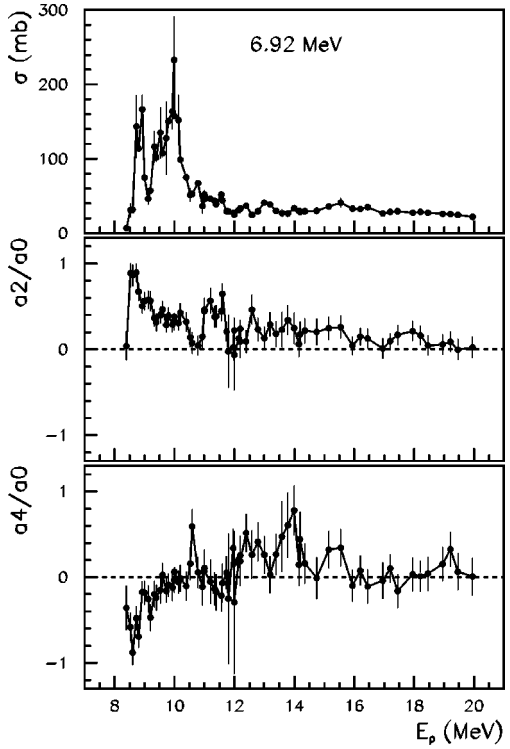

FIG. 4. Excitation function of the $^{16}O(p,p\gamma_{6.92})^{16}O$ reaction. Error bars are as explained in Fig. 3.

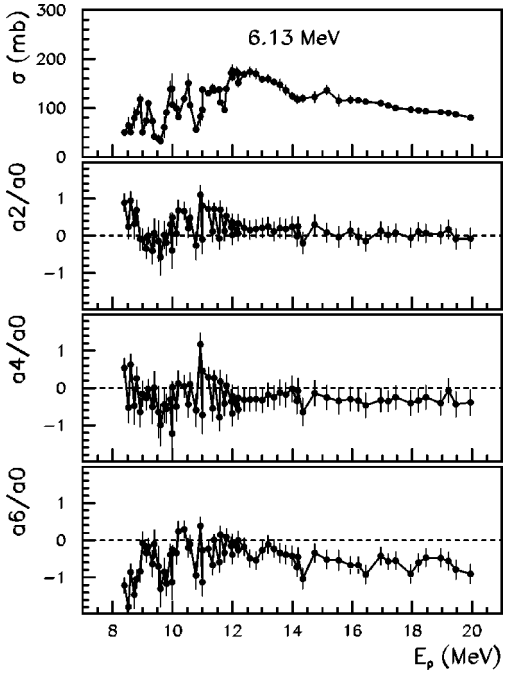

FIG. 5. Excitation function of the $^{16}O(p,p\gamma_{6.13})^{16}O$ reaction. Error bars are as explained in Fig. 3.

Lesko *et al.* [16] and Narayanaswamy *et al.* [17].

The 2.74 MeV γ-production cross section can be compared with the inelastic scattering cross section $^{16}O(p,p')^{16}O^*_{8.87}$ of Daehnick [20], measured between $E_p = 15.2$ and 19.2 MeV, taking into account the 77.7% branching ratio for the transition to the 6.13 MeV 3^- state [18]. Both measurements agree within 15% in the whole energy range, indicating negligible contributions from higher lying levels. Comparison of our 6.92+7.12 MeV data with the $^{16}O(p,p')^{16}O^*_{6.92+7.12}$ data of Daehnick, subtracting the contribution of the 8.87 MeV level to the 6.92 and 7.12 MeV γ rays in our data, shows an overall agreement of 15%, however, with some larger deviations up to 30% around 14 MeV and 40% between 15 and 16 MeV and at 16.5 MeV. This is probably due to contributions of higher lying levels, especially of the 0^- level at 10.95 MeV, which has a 100% branching to the 7.12 MeV level [19]. A corresponding 3.84 MeV γ ray is visible in our spectra, but hard to analyze due

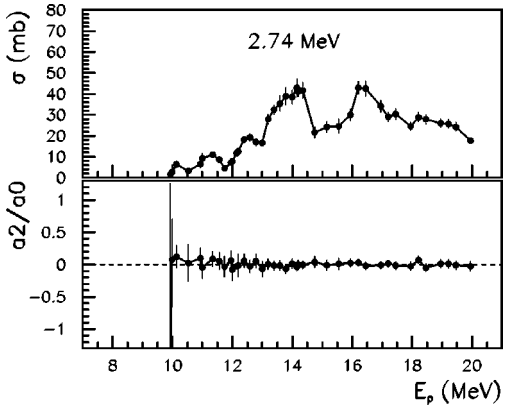

FIG. 6. Excitation function of the $^{16}O(p,p\gamma_{2.74})^{16}O$ reaction. Error bars are as explained in Fig. 3.

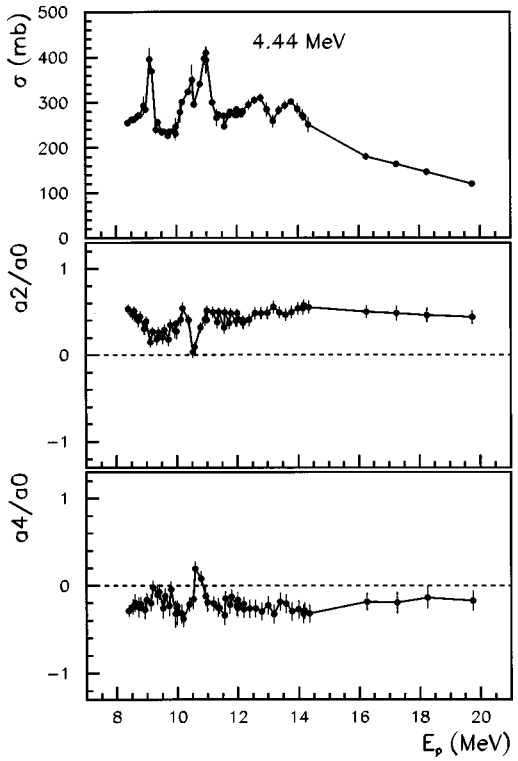

FIG. 7. Excitation function of the $^{12}C(p,p\gamma_{4.44})^{12}C$ reaction. Error bars are as explained in Fig. 3.

to high background and the vicinity of the first escape peak of the 4.44 MeV γ ray. Furthermore, it is probably confounded with a γ ray from $^{13}C(5/2^+, 3.854\ \text{MeV} \rightarrow \text{g.s.})$, induced by the $^{14}N(p,2p\gamma)^{13}C$ or the $^{13}C(p,p\gamma)^{13}C$ reaction. The cross section is in the several mb range above $E_p = 13$ MeV and does not exceed 15 mb. We did not compare with the measurements of Zobel *et al.* [21], since their 6.13 MeV γ-production cross sections deviate from all other measurements. These discrepancies are understood and discussed in more detail in [17,6].

In summary, the present data complete the excitation functions from inelastic proton scattering on ^{16}O in the energy range $E_p = 8.4$–20 MeV. Additionally, thanks to the carbon content in the used targets, γ-angular distributions for 4.44 MeV γ rays from inelastic proton scattering on ^{12}C have been obtained. In order to facilitate the use of the data in γ-ray astronomy, the data averaged over 1 MeV energy intervals are presented in Table I. For consistency, the cross section values for the 6.13 and 4.44 MeV γ-ray production have been directly taken from Dyer *et al.* In this paper β-delayed 4.44 MeV γ rays from the $^{12}C(p,n)^{12}N$ reaction are also included in the cross section, but this becomes only important at laboratory proton energies above 20 MeV (Q value $= -18.12$ MeV).

This work contributes an essential piece of nuclear input data for the production of the four strongest γ rays of ^{16}O and their line shape in low-energy cosmic rays interactions and in solar flares. Laboratory data from practically the threshold to 20 MeV proton energy are available for the 7.12, 6.92, and 2.74 MeV γ rays. A small part below 8.4 MeV of the γ-angular distribution is missing for the 6.13 MeV γ rays, but this fraction is negligible for line shape calculations in almost all realistic scenarios. Above $E_p = 20$ MeV, the inelastic scattering, at least for the levels with natural parity, is dominated by the direct reaction mechanism and can be relatively safely calculated by the distorted-wave Born approximation or by coupled channels approaches, as done for example in [6]. It is desirable to measure the same excitation functions for the inelastic α-particle scattering, which dominates the ^{16}O γ-ray production in astrophysical scenarios up to an accelerated particle energy of ≈ 8 MeV per nucleon, despite a lower helium abundance compared to hydrogen. Finally, it is equally important to complete the γ-angular distribution data for proton and α inelastic scattering on ^{12}C.

We would like to thank the operator crew of the IPN Orsay Tandem for their engagement and excellent preparation of the proton beam and the target service of the IPN Orsay for their help during the experiment.

TABLE I. Excitation functions for the $^{16}O(p,p\gamma)^{16}O$ and $^{12}C(p,p\gamma)^{12}C$ reactions. In the columns of $\sigma(6.13\ \text{MeV})$ and $\sigma(4.44\ \text{MeV})$ the values of the corresponding columns in Dyer *et al.* [9] were taken. The $a2/a0$ coefficient for the 2.74 MeV γ rays is not included in the table, since all values are compatible with zero.

E_p (MeV)	7.12 MeV		6.92 MeV			6.13 MeV				4.44 MeV			2.74 MeV
	σ (mb)	$a2/a0$	σ (mb)	$a2/a0$	$a4/a0$	σ (mb)	$a2/a0$	$a4/a0$	$a6/a0$	σ (mb)	$a2/a0$	$a4/a0$	σ (mb)
9	21	−0.04	93	0.58	−0.38	69	0.12	−0.17	−0.67	290	0.32	−0.17	0
10	37	−0.02	124	0.35	−0.06	97	0.28	−0.27	−0.32	265	0.36	−0.24	2.7
11	51	−0.08	50	0.27	0.07	122	0.49	0.07	−0.31	317	0.37	−0.10	7.8
12	39	−0.33	33	0.18	0.10	160	0.29	−0.27	−0.12	270	0.42	−0.22	10
13	45	−0.24	33	0.24	0.24	163	0.19	−0.27	−0.33	282	0.50	−0.26	23
14	58	−0.07	29	0.23	0.45	130	0.11	−0.23	−0.54	281	0.52	−0.28	39
15	54	0.04	34	0.23	0.20	128	0.13	−0.25	−0.49	217	0.54	−0.27	24
16	46	0.02	35	0.14	0.06	115	0.01	−0.34	−0.68	193	0.51	−0.21	34
17	41	0.05	29	0.08	−0.04	107	0.04	−0.35	−0.58	169	0.49	−0.19	34
18	33	0.15	28	0.17	−0.01	97	0.03	−0.33	−0.69	156	0.47	−0.16	27
19	30	0.08	26	0.05	0.16	92	0.06	−0.29	−0.54	140	0.45	−0.16	26

[1] R. J. Murphy, R. Ramaty, B. Kozlovsky, and D. V. Reames, Astrophys. J. **371**, 793 (1991).
[2] H. Bloemen *et al.*, Astron. Astrophys. **281**, L5 (1994); H. Bloemen *et al.*, Astrophys. J. Lett. **475**, L25 (1997).
[3] R. Ramaty, B. Kozlovsky, and R. E. Lingenfelter, Astrophys. J. Lett. **438**, L21 (1995); Astrophys. J. **456**, 525 (1996).
[4] E. Parizot, M. Cassé, and E. Vangioni-Flam, Astron. Astrophys. **328**, 107 (1997).
[5] R. Ramaty, B. Kozlovsky, and R. E. Lingenfelter, Astrophys. J., Suppl. **40**, 487 (1979).
[6] V. Tatischeff, M. Cassé, J. Kiener, J. P. Thibaud, and E. Vangioni-Flam, Astrophys. J. **472**, 205 (1996).
[7] A. M. Bykov, S. V. Bozhokin, and H. Bloemen, Astron. Astrophys. **307**, L37 (1996).
[8] B. Kozlovsky, R. Ramaty, and R. E. Lingenfelter, Astrophys. J. **484**, 286 (1997).
[9] P. Dyer, D. Bodansky, A. G. Seamster, E. G. Norman, and D. R. Maxson, Phys. Rev. C **23**, 1865 (1981).
[10] P. J. Nolan, F. A. Beck, and D. B. Fossan, Annu. Rev. Nucl. Part. Sci. **44**, 561 (1994).
[11] A. Coc, M. G. Porquet, P. Aguer, and J. P. Thibaud, Internal Report No. CSNSM 90-26, 1990 (unpublished).
[12] S. Messelt, Phys. Norv. **4**, 192 (1970).
[13] M. Pignanelli *et al.*, Phys. Rev. C **10**, 445 (1974).
[14] A. J. Ferguson, *Angular Correlation Methods in Gamma-Ray Spectroscopy* (North-Holland, Amsterdam, 1965).
[15] R. L. Dangle, L. D. Oppliger, and G. Hardie, Phys. Rev. **133**, B647 (1964).
[16] K. T. Lesko, E. B. Norman, R.-M. Larimer, S. Kuhn, D. M. Meekhof, S. G. Crane, and H. G. Bussell, Phys. Rev. C **37**, 1808 (1988).
[17] J. Narayanaswamy, P. Dyer, S. R. Faber, and S. M. Austin, Phys. Rev. C **24**, 2727 (1981).
[18] D. R. Tilley, H. R. Weller, and C. M. Cheves, Nucl. Phys. **A564**, 1 (1993).
[19] R. B. Firestone, *Table of Isotopes*, 8th ed., edited by V. S. Shirley (Wiley, New York, 1996).
[20] W. W. Daehnick, Phys. Rev. **135**, B1168 (1964).
[21] W. Zobel, F. C. Maienschein, J. H. Todd, and G. T. Chapman, Nucl. Sci. Eng. **32**, 392 (1968).